Hydrogen- and Halogen-Bonds between Ions of like Charges: Are They Anti-Electrostatic in Nature?

Changwei Wang,*[a] Yuzhuang Fu,[a] Lina Zhang,[a] David Danovich,[b] Sason Shaik ,*[b] and Yirong Mo *[c]

Recent theoretical studies suggested that hydrogen bonds between ions of like charges are of a covalent nature due to the dominating $n_D \rightarrow \sigma^*_{H\text{-}A}$ charge-transfer (CT) interaction. In this work, energy profiles of typical hydrogen (H) and halogen (X) bonding systems formed from ions of like charges are explored using the block-localized wavefunction (BLW) method, which can derive optimal geometries and wave functions with the CT interaction "turned off." The results demonstrate that the kinetic stability, albeit reduced, is maintained for most investigated systems even after the intermolecular CT interaction is quenched. Further energy decomposition analyses based on the BLW method reveal that, despite a net repulsive Coulomb repulsion, a stabilizing component exists due to the polarization effect that plays significant role in the kinetic stability of all systems. Moreover, the fingerprints of the augmented electrostatic interaction due to polarization are apparent in the variation patterns of the electron density. All in all, much like in standard H- and X-bonds, the stability of such bonds between ions of like charges is governed by the competition between the stabilizing electrostatic and charge transfer interactions and the destabilizing deformation energy and Pauli exchange repulsion. While in most cases of "anti-electrostatic" bonds the CT interaction is of a secondary importance, we also find cases where CT is decisive. As such, this work validates the existence of anti-electrostatic H- and X-bonds. © 2017 Wiley Periodicals, Inc.

DOI: 10.1002/jcc.25068

Introduction

Hydrogen bonding (H-bonding) is a core concept for noncovalent interactions; it is of great importance not only in chemistry but also in molecular biology and material science.[1–5] H-bond can be represented as D···H – A, where D is the acceptor having electron rich center(s), and H – A is the donor possessing a positively charged H atom. H-bonding properties, such as the cooperative effect and directionality have been extensively investigated. Based on current understanding, the electrostatic attraction between the electron-deprived hydrogen and the electron-rich center on D plays the key role in H-bonding,[6,7] while the charge-transfer (CT) from D to the antibonding σ^* orbital of H–A (i.e., $n_D \rightarrow \sigma^*_{H\text{-}A}$), which brings about covalence, is also important and largely responsible for the directionality of the hydrogen bond.[8–15] While many new types of strong and unconventional H-bonds have been identified and recognized, some initially unexpected forms of H-bonding, such as the B – H···π hydrogen bond,[16] or the hydrogen bond between positively charged phosphorus and hydrogen atoms,[17] or even hydrogen bonds between ions of like charge,[18–21] have also been experimentally observed. These recent and novel studies enrich the categories of H-bonds, and call for a more profound and comprehensive theoretical treatment of H-bonding.

Our interest here lies is in the H-bonding between H-donor and -acceptor of like charges,[18–25] such as the recent experimentally observed OH···P H-bonding.[17] The existence of such a complex seemingly violates the electrostatic paradigm of H-bonding, as ions of like charges must be mutually repulsive. However, according to the computational analyses by Kjaergaard et al., the net-positively charged P atom possesses an area on the electron density surface with a negative electrostatic potential, which attracts the positively charged H atom and thereby forms the H-bond.[17] Obviously, this theoretical model of Kjaeraard et al. espouses an electrostatic explanation, which is similar but in opposite sense to the σ-hole concept coined by Politzer et al.[26,27] As such, the term "σ-cusp" may be accordingly introduced to describe the negative electrostatic potential area crowned by positive potentials.

An early example of H-bonding between ions of like charge is the $(O\text{–}H)^-\cdots O^-$ system, observed experimentally by Braga et al.[18] Theoretical investigations based on the quantum theory

[a] C. Wang, Y. Fu, L. Zhang
Department of Chemistry, College of Science, China University of Petroleum (East China), Changjiangxi Road 66, 266580 Tsingtao, China
E-mail: upc.changweiwang@gmail.com
[b] D. Danovich, S. Shaik
Institute of Chemistry, The Hebrew University, Jerusalem 91904, Israel
E-mail: sason@yfaat.ch.huji.ac.il
[c] Y. Mo
Department of Chemistry, Western Michigan University, Kalamazoo, Michigan 49008
E-mail: ymo@wmich.edu
Contract grant sponsor: Natural Science Foundation of China (to C.W.); Contract grant number: 21603274; Contract grant sponsor: Fundamental research funds for the central Universities; Contract grant number: 15CX05066A; Contract grant sponsor: China University of Petroleum; Contract grant number: 2014010575; Contract grant sponsor: ISF (to SS); Contract grant number: 1183/13; Contract grant sponsor: Faculty Research and Creative Activities Award (FRACAA), Western Michigan University (WMU)

of atoms in molecules (QTAIM) method[28] by Macchi et al. suggested that the H-bonding is contributed here by both CT interaction and electrostatic attraction.[29] Most recently, Alkorta et al.[30] investigated neutral and charged carboxylic acid dimers, and found that the carboxylate-ion dimers are similar to their neutral counterparts; having no significant difference in their electron density distribution as well as their electric-field maps.[30] Interestingly, by decomposing the total molecular energy to interatomic and intra-atomic terms within the QTAIM method, they demonstrated that the interaction between the carboxylic groups in both neutral and ionic complexes is always attractive, though the total intermolecular electrostatic interaction in the ionic complexes is repulsive as expected.[30] Thus, the dominance of electrostatic attraction seems universal in all kinds of H-bonds, though the covalence must not be neglected, as it is associated with the directionality of H-bonds.

This coexistence of electrostatics and covalence in H-bonding, however, was challenged by Weinhold and Klein who proposed the concept of "anti-electrostatic" H-bond (AEHB), for example, in $[F^{-}\cdots HCO_3]^{2-}$.[31] Despite the overall repulsive binding energy, the kinetic stability, which is characterized by a local minimum on the energy profile along the D···H–A distance, were confirmed in H-bonding complexes formed by ions of like charges.[31] These unusual H-bonds seem to be perfect counter-examples of the popular electrostatic explanation, because both the H-bond donor and acceptor are ions having like charges, suggesting an overall Coulomb repulsion and hence irrelevance of the electrostatic explanation in standard H-bonds. Moreover, the considerable covalent nature of "AEHB" was ascribed to a strong $n_D \rightarrow \sigma^*_{H\text{-}A}$ CT interaction, based on natural bond orbital (NBO) analysis.[32,33] This novel proposal of AEHB instantly stimulated heated discussions.[34,35] The exemplary $[F^{-}\cdots HCO_3]^{2-}$ dianion was re-examined by Frenking and Caramori, who proved the Coulombic force as the secondary significant stabilizing factor, despite the dominating orbital interaction.[34] Since any unusual and controversial idea is also beguiling, we were prompted to carry out a more detailed investigation of the compatibility of AEHB with the conventional theory on H-bonding and furthermore on halogen bonding (X-bonding).

The term X-bonding refers to the interaction between a halogen atom X and an electron-rich center of D in a D···X – A complex. X-bonds have attracted enormous attentions in chemistry, biology and material science.[36–45] Similarities in both strength and properties between H- and X-bonds were observed.[46,47] Moreover, cases were found where H- and X-bonds compete with each other.[26,48–52] Notably, much like H-bonding, X-bonding also involves both partial covalent and electrostatic interactions.[53,54] As such, the X-bond can be similarly explained by the electrostatic attraction between the electron-rich center on D, and the "σ-hole," which is a region with positive electrostatic potential around the halogen atom pointing along the extension of the A – X bond.[26,27,55,56] All these similarities between H- and X-bonds call for a parallel investigation, which should address the following intriguing question: *do X-bonding systems exist between ions of like charges, as found for H-bonds, and do these X- and H-bonds possess kinetic stability?*

In fact, some "anti-electrostatic" X-bonds ("AEXB") were already observed experimentally. Walbaum et al. showed that the tetra(diiodine)chloride ($[Cl(I_2)_4]^{-}$) dimer exhibits kinetic stability.[57] Similarly, Martí-Rujas et al.[58] made the tetrahalide anion $[I_2Cl_2]^{2-}$, and found it to be a linear complex, $Cl^{-}\cdots I_2\cdots Cl^{-}$, involving X-bonds between a central I_2 molecule and two Cl^{-}anions. This X-bonding $Cl^{-}\cdots I_2\cdots Cl^{-}$ has also been utilized subsequently in a supermolecular assembly.[59] In spite of the electric neutrality of I_2 molecule, the pinning Cl^{-} anions on each side suggest a repulsive electrostatic interaction and a potential "AE" feature. Most recently, the stability and characteristics of AEXB were studied computationally by Wang et al. and Quiñonero et al.[60,61] Obviously, a comparative study of the existence of "AE" in X- and H-bonds would be relevant to experimental cases.

For the sake of convenience, here, we use the notation D···Y–A (Y = H or X) to generalize both H-bonds and X-bonds, where D represents a Lewis base, and Y – A is a Lewis acid acting as the H- or X-bond donor. We generate energy profiles of certain H- and X-bonds between ions of like charges, and explore them using the block-localized wavefunction (BLW) method,[62–65] which is a variant of the valence bond (VB) theory.[66–69] The BLW method can uniquely "turn off" intermolecular CT interaction, and thus directly verify the role of covalence in the so-called "AE" phenomena. In addition, both the direct electrostatic interaction and the polarization effect between the two ions will be examined and compared with the charge-transfer interaction. Finally, a unified explanation for the "AE" phenomena in both H- and X-bonds will be proposed.

Theoretical Backgrounds

The BLW method and its energy decomposition (BLW-ED) approach

The BLW method defines an electron-localized state with block-localized MOs, which are expanded only in a subset of the whole basis functions, belonging to either D or YA. Orbitals in the same subset are subject to the orthogonality constraint while orbitals among different subsets are generally nonorthogonal. For the D···Y – A (Y = H or X) complex, the electron-localized intermediate state can be conveniently defined as

$$\Psi^{BLW0} = \hat{A}\left(\Psi_D^0 \Psi_{YA}^0\right) \quad (1a)$$

$$\Psi^{BLW} = \hat{A}\left(\Psi_D \Psi_{YA}\right) \quad (1b)$$

where Ψ^{BLW0} is the zero-order electron-localized wavefunction constructed with the optimal wavefunctions of separated D and YA at the geometries in the complex, while Ψ^{BLW} is self-consistently optimized. The BLW method has been successfully extended to the DFT level[63] with Grimme's dispersion correction.[70,71]

The nature of noncovalent interactions can be explored with the BLW energy decomposition (BLW-ED) approach. In the BLW-ED approach, the binding energy is composed of two terms, one refers to the energy cost for changing the monomers from their isolated optimal geometries to those in the optimal complex

(ΔE_{def}), and the other measures the interaction between two monomers with geometries frozen (ΔE_{int}):

$$\Delta E_b = \Delta E_{def} + \Delta E_{int} \quad (2)$$

The interaction energy can be further decomposed to a number of energy components as

$$\Delta E_{int} = E(\Psi_{DYA}) - [E(\Psi_D) + E(\Psi_{YA})] + BSSE = \Delta E_F + \Delta E_{pol} + \Delta E_{CT} + \Delta E_{disp} \quad (3)$$

where ΔE_F is the frozen energy term, in which D and YA form the complex without altering their individual electron densities, and BSSE refers to the basis set superposition error and is computed with the Boys and Bernardi counterpoise method.[72] Note that ΔE_F involves not only the Pauli repulsion between D and YA, but also the electrostatic interaction that plays a key role in the "AE" phenomenon. The term ΔE_{pol} reflects the redistribution of electron density within D and YA due to the electric field they exert on one another. Hence, this term is a stabilizing force, and so is the charge transfer energy ΔE_{CT} which is the energy difference between the optimized electron-localized state $E(\Psi^{BLW})$, and the electron-delocalized state ($E(\Psi^{MO})$), with the BSSE correction. The difference in Grimme's dispersion correction between the whole complex (E^{Tot}_{disp}) and the sum of each monomer (E^{i}_{disp}, i = A and B) is defined as the dispersion energy (ΔE_{disp}). Exact definitions of these energy terms are

$$\Delta E_F = E(\Psi^{BLW0}) - [E(\Psi^0_A) + E(\Psi^0_B)] \quad (4a)$$

$$\Delta E_{pol} = E(\Psi^{BLW}) - E(\Psi^{BLW0}) \quad (4b)$$

$$\Delta E_{CT} = E(\Psi^{MO}) - E(\Psi^{BLW}) + BSSE \quad (4c)$$

$$\Delta E_{disp} = E^{Tot}_{disp} - E^{A}_{disp} - E^{B}_{disp} \quad (4d)$$

Often, we prefer to interpret chemistry in stereoelectronic terms. Thus, the charge transfer (CT) term is the one that brings about covalent bonding between the interacting moieties, whereas the steric effect involves the rest of the energy components in the binding energy, as follows:

$$\Delta E_s = \Delta E_{def} + \Delta E_F + \Delta E_{pol} + \Delta E_{disp} \quad (5)$$

$$\Delta E_b = \Delta E_s + \Delta E_{CT} \quad (6)$$

Both the geometry optimization and vibrational frequency calculations of electron localized states can be achieved using the in-house version of GAMESS software,[73] which makes the exploration of diabatic energy profiles available. Consequently, the role of charge transfer interaction in the "AE" phenomenon can be directly examined by comparing the regular DFT and BLW energy profiles.

Computational details

In line with earlier studies, the present study focuses on four typical examples of "AE" H-bonding systems as shown in Figures 1a–1d. Both the bioxalate and p-biphthalate dimers[31]

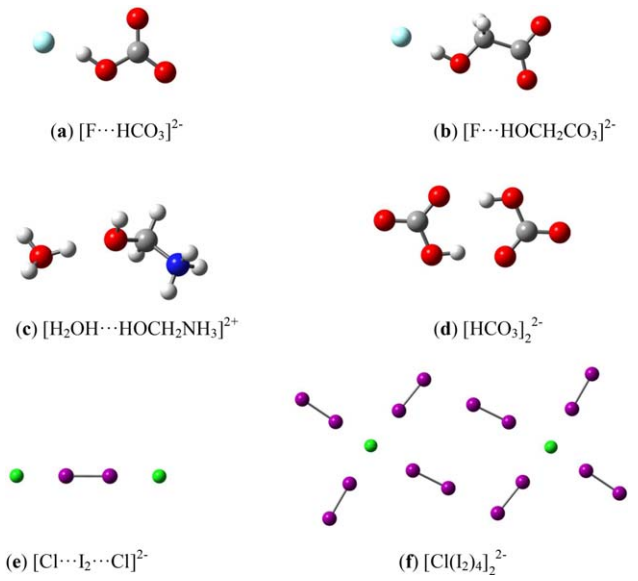

Figure 1. Model H- and X-bonding complexes investigated in this work. Carbon, oxygen, nitrogen, and hydrogen atoms are represented with gray, red, blue, and white balls, respectively, whereas fluorine, chlorine, and iodine are represented with cyan, green, and purple balls. [Color figure can be viewed at wileyonlinelibrary.com]

are not considered as they are analogous to the bicarbonate dimer (Fig. 1d) and all are formed by antiparallel H-bonding between carboxylate groups in C_2-symmetry. Instead, we include $[Cl\cdots I_2\cdots Cl]^{2-}$ and $[Cl(I_2)_4]^-$ dimer as X-bonding systems (Figs. 1e and 1f).

The M06-2X functional,[74] which has been proven reliable for various kinds of noncovalent interactions,[75,76] is adopted here, and is augmented with Grimme's dispersion correction.[70,71] Energy profiles along the bonding distance in D···Y–A distance has been explored at this M06-2X-D3/cc-pVTZ level of theory. At each point of energy profiles, all geometrical parameters except the bonding distance (reaction coordinate) were optimized. Positive binding energies and local minima on energy profiles have been found for all systems (Supporting Information Fig. S1), indicating the likely existence of the "AE" phenomena in all these target H- and X-bonding systems. We have also explored the energy profiles of systems **a**-**e** at the SCSMP2/aug-cc-pVTZ level,[77,78] and computed the binding energies at the CCSD(T)/aug-cc-pVTZ level with the BSSE corrected (Supporting Information Fig. S1). The CCSD(T) results confirm the existence of "AE" in all systems except **a**, for which an unconventional interval (from 1.8 to 2.1 Å), where the CCSD(T) curve is flat, has been found, in spite of the absence of the kinetic stability (which may qualify **a** as a persistent species). For systems **b–e**, the sequence of the well depths (energy differences between local maxima and minima) is predicted correctly (**c** < **d** < **b** < **e**) at the M06-2X-D3/cc-pVTZ level with references to the CCSD(T) results, although the absolute values are overestimated to some extent. At last, the optimal Cl···Cl distance in complex **f** is 12.2 Å (Supporting Information Table S1), or only 0.210 Å longer than the value obtained at the SCSMP2/def2-TZVPP level of theory.[57] In general, the M06-2X-D3/cc-pVTZ level, adopted in the present

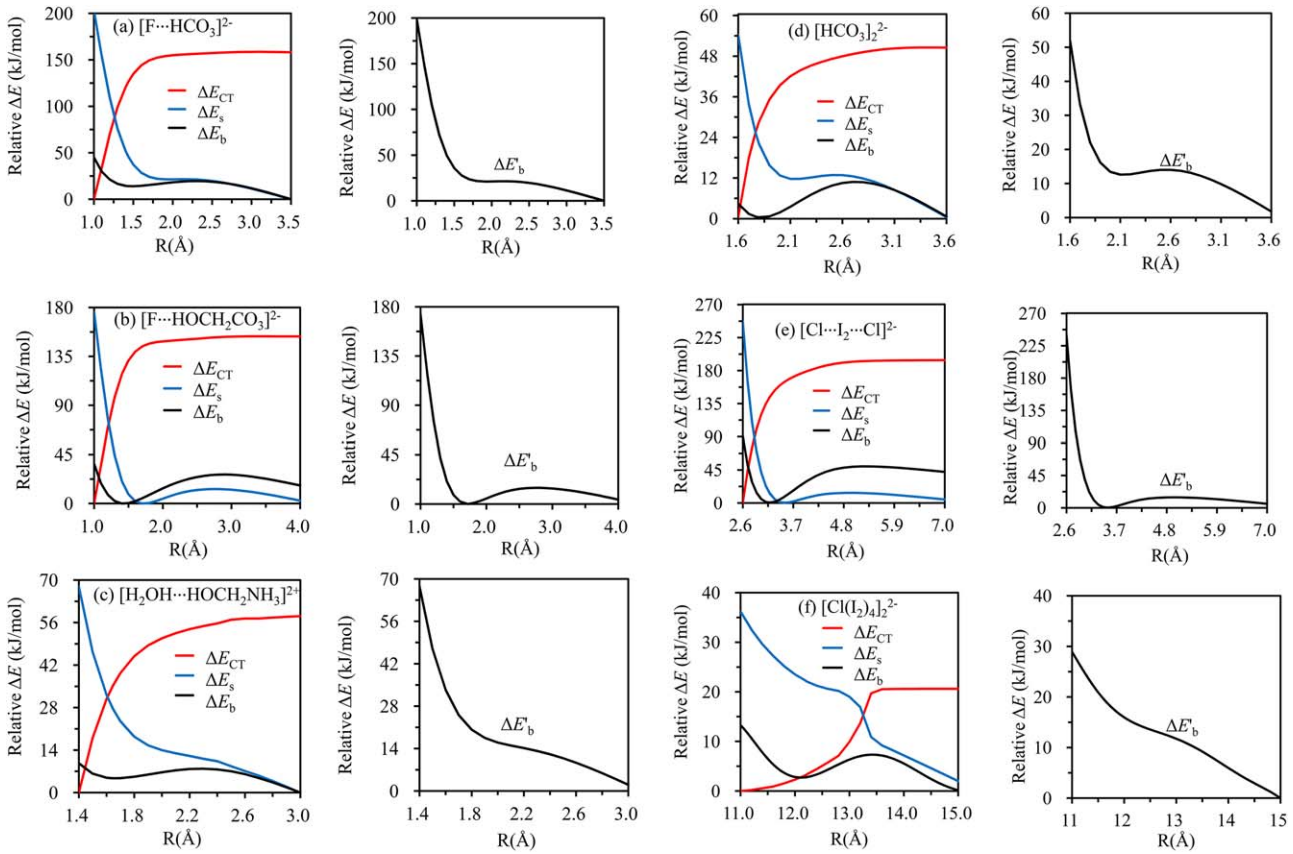

Figure 2. Energy profiles with the variation of the D···Y – A bond distance (R). Left curves are based on the regular DFT optimal geometries while the right curves are based on the BLW optimal geometries. [Color figure can be viewed at wileyonlinelibrary.com]

study, provides us reliable results for both H- and X-bonding systems with "AE" characteristic. Definitions of blocks for electron-localized states are shown in Supporting Information Figure S2.

Results and Discussion

The essential characteristic of the "AE" phenomenon is the attractive local minimum on the potential energy surface, which "traps" the complex and ensures its kinetic persistence, although the overall contact is energetically unfavorable. Hence, the energy profiles derived from regular DFT computations have been analyzed by decomposing the binding energy into CT energy (ΔE_{CT}) and steric energy (ΔE_s) as shown in eq. (6), to verify the role of CT in the formation of the attractive minima on energy profiles. Energy profiles with diabatic geometries optimized using the BLW methods have also been obtained for comparison.

Analytical results of these energy profiles are shown in Figure 2 and two findings can be noted based on the energy profiles with regular DFT geometries. First, the CT interaction is invariably enhanced as the intermolecular distance decreases, indicating a universal binding contribution to local minima. This is understandable as the overlap between the lone pair orbital on D and the virtual orbital $\sigma^*_{Y\text{-}A}$ on Y–A constantly increases with the shortening of the bonding distance. Second, local minima on the steric energy curves are shallower (or even fading away in systems **a**, **c**, and **f**), compared with those on their corresponding binding energy curves, where the CT interaction is included. These two observations suggest a significant and sometimes decisive role of the CT interaction in the "AE" phenomenon in both H- and X-bonds.

Nevertheless, the energy profiles with diabatic geometries where the CT interaction is quenched ($\Delta E'_b$ curves in Fig. 2) show that the minima still exist for most of the systems except **c** and **f**. Comparison of energy profiles (ΔE_b vs. $\Delta E'_b$ in Fig. 2) indicates that the intermolecular CT interaction indeed plays a significant role in the "AE" phenomenon. Notably, $\Delta E'_b$ curves for system **c** and **f** keep increasing as the bond distances decrease, implying the decisive role of the CT interaction in their "AE" phenomena. For **a**, there is a very shallow well in the $\Delta E'_b$ curve, as its depth is only 0.4 kJ/mol and essentially the interval from 1.8 Å to 2.3 Å can be taken as a horizontal line. As such, the CT interaction in **a** is also critical for the existence of a local minimum on the energy surface, or the existence of the "AE" phenomenon.

Having proved that the CT interaction is decisive for the appearance of minima in the energy profiles of **c** and **f**, we continue to explore the origin of the attractive minima for the rest of the complexes (**a**, **b**, **d**, and **e**). Table 1 lists the energy contributions to the well depths (in negative values to reflect the stability with references to local maxima) for the electron-localized states ($\Delta E'_b$) wherein the CT interaction is quenched. The respective minima for **a**, **b**, and **d**, are solely governed by the polarization interaction, while the

Table 1. Contributions of each component (in kJ/mol) to the well depth, based on the energy profiles of the electron localized state.

Complex	$\Delta E'_{def}$	$\Delta E'_{F}$	$\Delta E'_{pol}$	$\Delta E'_{disp}$	$\Delta E'_{b}$
a	3.5	4.0	−7.9	0.0	−0.4
b	3.8	11.5	−30.1	0.0	−14.8
d	2.8	3.2	−7.9	0.0	−1.9
e	1.0	−5.3	−10.0	0.0	−14.3

Molecular structure Polarization Charge transfer.

destabilizing deformation and frozen energy oppose polarization. For system **e**, there is a considerable contribution from the frozen energy (–5.3 kJ/mol), yet the polarization interaction plays the dominant role and contributes 70.0% of the overall well depth. Thus, the stabilizing polarization interaction is an important factor for the "AE" phenomenon in systems **a**, **b**, **d**, and **e**. This finding is sound because the electric field imposed by one monomer on the other, is enhanced as the distance between the monomers get closer (i.e., from local maxima to minima), resulting in a more favorable electrostatic attraction. On the other hand, the shortening of H- or X-bonding distances leads to an enhanced destabilizing Pauli exchange repulsion, which subsequently flattens the energy well. This can be exhibited by the energy decomposition analysis of the energy profiles at the diabatic geometries as shown in Supporting Information Figure S3. The polarization interaction is strengthened continuously as the H- or X-bonding distance shortens, while the

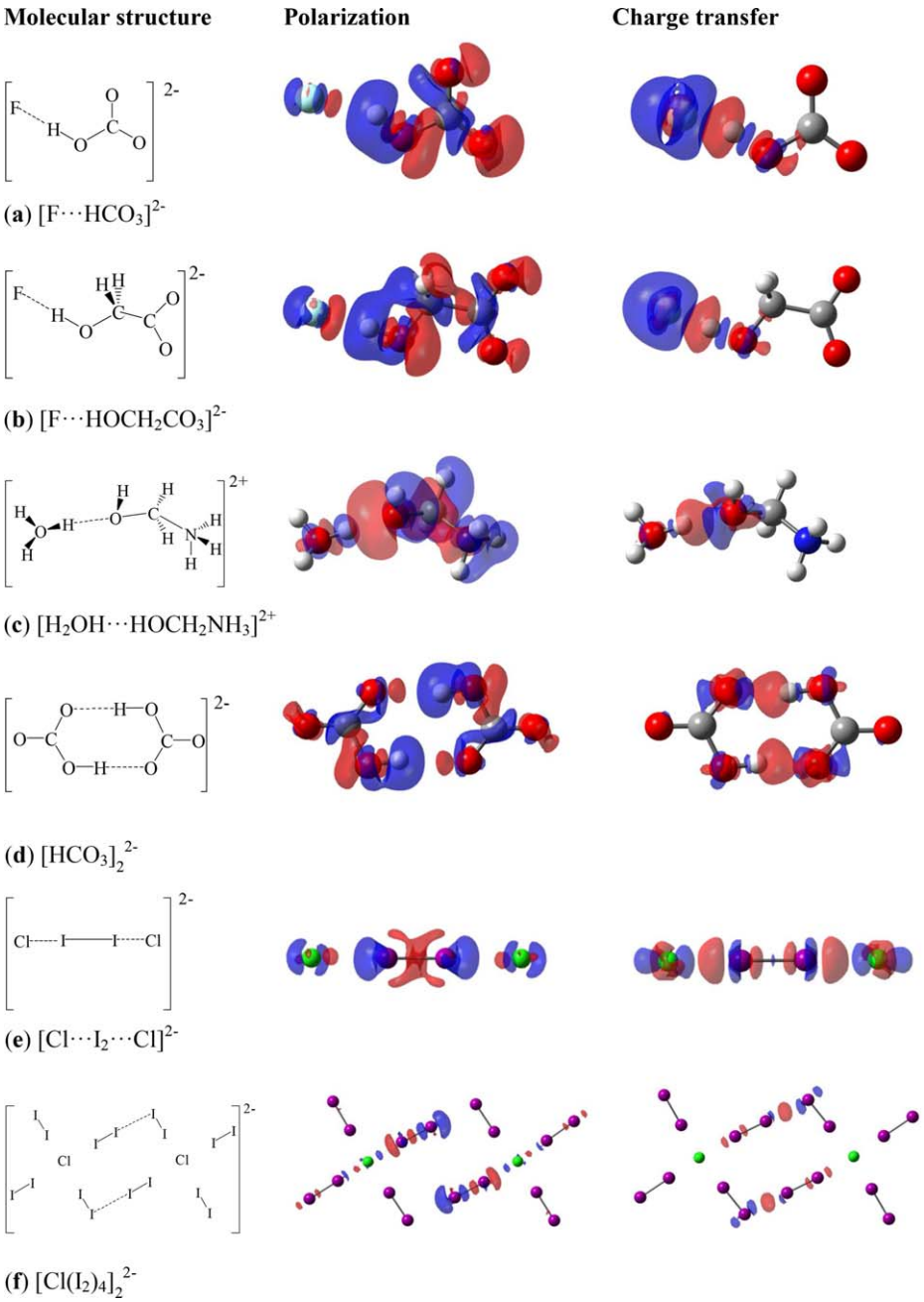

Figure 3. Electron density difference (EDD) maps due to the polarization effect (middle column) and charge transfer interaction (left column) in all systems **a–e**; a blue color means enhanced density, while a red color denotes depleted density. [Color figure can be viewed at wileyonlinelibrary.com]

Table 2. Contributions of each component (in kJ/mol) to the well depth, based on the energy profiles of the electron delocalized state.

Complex	ΔE_{def}	ΔE_F	ΔE_{pol}	ΔE_{CT}	ΔE_{disp}	ΔE_b
a	33.3	41.1	−49.9	−29.9	0.0	−5.4
b	23.3	53.6	−68.4	−35.2	0.0	−26.6
c	5.0	36.4	−25.1	−19.5	0.0	−3.2
d	16.8	26.4	−30.8	−22.8	0.1	−10.3
e	8.1	10.3	−17.6	−50.1	0.0	−49.4
f	5.9	9.9	−3.7	−17.0	−0.2	−5.1

curves of the destabilizing deformation and frozen energies move up except for system **e**. We note that the contribution from the dispersion interaction is negligible for all cases (Table 1) and thus can be ignored.

To appreciate the polarization effect intuitively, electron density difference (EDD) maps representing the electron density variation due to the polarization interaction are shown in Figure 3 (middle column), based on the BLW optimal geometries. In all cases, there is an electron density movement on D from the far end to the near end towards the bonding partner YA. For instance, the electron density flows from the left side (far end) of the F^- anion, to its right side, which is region involved in bonding, for both complexes **a** and **b**. Similar pattern of electron density variation can also be observed in the other cases. Meanwhile, electron densities on YA move from the Y side to the A side. These correlated charge-polarization modes enhance the ensuing electrostatic attraction.

Binding energies at the optimal geometries of electron-delocalized states were also analyzed with the BLW-ED method and compiled in Table 2. Compared with Table 1, both the deformation and frozen energy contributions become more significant and play adverse roles in the establishment of the "AE" phenomenon. This is simply due to the significant shortening of the bonding distances occurring when the CT interaction is "turned on." The shortening of the H- or X-bonding distances (compared with their lengths in the BLW states) causes stronger destabilizing Pauli repulsions between the monomers and greater distortion energy due to their geometric deformations.

We stress that the CT interaction contributes significantly to the well depths in the energy profiles of all H- and X-bonds of ions of like charges. In many cases, it plays the secondary role for "AEHBs" after the polarization effect, which is electrostatic in nature, but in certain cases such as **f**, CT is indeed decisive. Further, for both "AE" X-bonding complexes **e** and **f**, the CT interaction is the most important energy component the kinetic stability. This observation is consistent with the CT nature of X-bonds,[54] and supports the "AE" nature of the kinetic stability. Interestingly, the well on the energy profile of system **e** remains, even after quenching the CT interaction, but for system **f**, quenching the CT interaction erases the well on the respective energy profile. The EDD maps showing the electron density variation caused by the CT interaction are also presented in Figure 3. A reduction of electron density on the binding site of Y, and an accumulation of electron density in the binding area between monomer can be observed. This pattern of electron density variation is the same as in conventional H- or X-bonding systems studied previously.

Concluding Remarks

The kinetic stability of H- and X-bonds between ions of like charge is confirmed by the energy profiles explored at the CCSD(T)/aug-cc-pVTZ level of theory, using the geometries optimized at the SCSMP2/aug-cc-pVTZ level of theory. For D···Y–A (Y = H or X) complexes, the CT interaction between D and Y–A gauges the covalence which contributes to the emerging "AE" phenomenon in both H-bond or X-bond. To quantify the CT interaction, we employed the BLW method, which generates self-consistently optimized electron-localized states where the CT interaction is quenched. Computations of six exemplary H-bonding and X-bonding systems show that indeed, for several complexes such as **c** and **f** in Figure 1, the CT interaction is truly decisive in the formation of wells on the respective total energy profiles. For others, the CT interaction, while not dominant, still plays an important role. Thus, in general the present study validates the concept of AEHB though it is not universal.

Further energy decomposition analyses of the energy profiles with diabatic structures show that, the stabilizing polarization interaction plays a significant role for the well depth in all cases, while both frozen and deformation energies tend to flatten the wells. We note that the polarization stabilization is of electrostatic nature. In addition, a loss of electron density on Y and a gain of electron density on the binding site of D are observed on the EDD maps showing the electron density flow due to polarization interaction, suggesting a strengthened electrostatic interaction.

Keywords: valence bond theory · block-localized wavefunction · energy decomposition analysis · anti-electrostatic hydrogen bond · anti-electrostatic halogen bond

How to cite this article: C. Wang, Y. Fu, L. Zhang, D. Danovich, S. Shaik, Y. Mo. *J. Comput. Chem.* **2018**, *39*, 481–487. DOI: 10.1002/jcc.25068

Additional Supporting Information may be found in the online version of this article.

[1] S. Scheiner, *Hydrogen Bonding*; Oxford University Press: New York, **1997**.
[2] G. A. Jeffrey, *An Introduction to Hydrogen Bonding*; Oxford University Press: New York, **1997**.
[3] M. Nishio M. Hirota, Y. Umezawa, *The CH/π Interaction: Evidence, Nature, and Consequences*; Wiley-VCH: New York, **1998**.
[4] G. Gilli, P. Gilli, *The Nature of the Hydrogen Bond: Outline of a Comprehensive Hydrogen Bond Theory*; Oxford University Press: New York, **2009**.
[5] G. R. Desiraju, *Acc. Chem. Res.* **2002**, *35*, 565.
[6] L. C. Pauling, *The Nature of the Chemical Bond*, 3rd ed; Cornell University Press: Ithaca, NY, **1960**.
[7] K. Morokuma, *Acc. Chem. Res.* **1977**, *10*, 294.
[8] P. A. Kollman, L. C. Allen, *Chem. Rev.* **1972**, *72*, 283.
[9] S. Y. Liu, C. E. Dykstra, *J. Phys. Chem.* **1986**, *90*, 3097.
[10] M. S. Gordon, J. H. Jensen, *Acc. Chem. Res.* **1996**, *29*, 536.

[11] T. K. Ghanty, V. N. Staroverov, P. R. Koren, E. R. Davidson, *J. Am. Chem. Soc.* **2000**, *122*, 1210.
[12] C. L. Perrin, *Acc. Chem. Res.* **2010**, *43*, 1550.
[13] S. Grabowski, *J. Chem. Rev.* **2011**, *111*, 2597.
[14] H. Hirao, X. Wang, In *The Chemical Bond*; G. Frenking, S. Shaik, Eds.; Wiley VCH: Weinheim, **2014**; pp. 501–522.
[15] N. Mohan, C. H. Suresh, *J. Phys. Chem. A* **2014**, *118*, 1697.
[16] X. Zhang, H. Dai, H. Yan, W. Zou, D. Cremer, *J. Am. Chem. Soc.* **2016**, *138*, 4334.
[17] A. S. Hansen, L. Du, H. G. Kjaergaard, *J. Phys. Chem. Lett.* **2014**, *5*, 4225.
[18] D. Braga, F. Grepioni, J. J. Novoa, *Chem. Commun.* **1998**, 1959.
[19] W. Gamrad, A. Dreier, R. Goddard, K.-R. Pörschke, *Angew. Chem. Int. Ed.* **2015**, *54*, 4482.
[20] I. Mata, I. Alkorta, E. Molins, E. Espinosa, *Chem. Phys. Lett.* **2013**, *555*, 106.
[21] I. Mata, E. Molins, I. Alkorta, E. Espinosa, *J. Phys. Chem. A* **2015**, *119*, 183.
[22] S. W. Lee, J. L. Beauchamp, *J. Am. Soc. Mass. Spectrom.* **1999**, *10*, 347.
[23] L. Feketeova, R. A. O'Hair, *J. Chem. Commun.* **2008**, *2008*, 4942.
[24] S. R. Kass, *J. Am. Chem. Soc.* **2005**, *127*, 13098.
[25] I. Mata, I. Alkorta, E. Molins, E. Espinosa, *ChemPhysChem* **2012**, *13*, 1421.
[26] P. Politzer, J. S. Murray, P. Lane, *Int. J. Quantum Chem.* **2007**, *107*, 3046.
[27] T. Clark, M. Hennemann, J. S. Murray, P. Politzer, *J. Mol. Model.* **2007**, *13*, 291.
[28] R. F. W. Bader, *Atoms in Molecules: A Quantum Theory*; Oxford University Press: Oxford, UK, **1990**.
[29] P. Macchi, B. B. Iversen, A. Sironi, B. C. Chakoumakos, F. K. Larsen, *Angew. Chem. Int. Ed.* **2000**, *39*, 2719.
[30] I. Alkorta, I. Mata, E. Molins, E. Espinosa, *Chemistry* **2016**, *22*, 9226.
[31] F. Weinhold, R. A. Klein, *Angew. Chem.* **2014**, *126*, 11396.
[32] F. Weinhold, C. R. Landis, In *Discovering Chemistry with Natural Bond Orbitals*; Wiley, **2012**; pp. 209–230.
[33] A. E. Reed, L. A. Curtiss, F. Weinhold, *Chem. Rev.* **1988**, *88*, 899.
[34] G. Frenking, G. F. Caramori, *Angew. Chem. Int. Ed.* **2015**, *54*, 2596.
[35] F. Weinhold, R. A. Klein, *Angew. Chem. Int. Ed.* **2015**, *54*, 2600.
[36] P. Auffinger, F. A. Hays, E. Westhof, P. S. Ho, *Proc. Natl. Acad. Sci. USA* **2004**, *101*, 16789.
[37] R. Bertani, P. Sgarbossa, A. Venzo, F. Lelj, M. Amati, G. Resnati, T. Pilati, P. Metrangolo, G. Terraneo, *Coord. Chem. Rev.* **2010**, *254*, 677.
[38] L. A. Hardegger, B. Kuhn, B. Spinnler, L. Anselm, R. Ecabert, M. Stihle, B. Gsell, R. Thoma, J. Diez, J. Benz, J.-M. Plancher, G. Hartmann, D. W. Banner, W. Haap, F. Diederich, *Angew. Chem. Int. Ed.* **2011**, *50*, 314.
[39] A. C. Legon, *Phys. Chem. Chem. Phys.* **2010**, *12*, 7736.
[40] D. Mani, E. Arunan, *Phys. Chem. Chem. Phys.* **2013**, *15*, 14377.
[41] G. Mínguez Espallargas, F. Zordan, L. Arroyo Marín, H. Adams, K. Shankland, J. van de Streek, L. Brammer, *Chemistry* **2009**, *15*, 7554.
[42] A. J. Parker, J. Stewart, K. J. Donald, C. A. Parish, *J. Am. Chem. Soc.* **2012**, *134*, 5165.
[43] F. Meyer, P. Dubois, *CrystEngComm* **2013**, *15*, 3058.
[44] H. Haller, S. Riedel, *Z. Anorg. Allg. Chem.* **2014**, *640*, 1281.
[45] S. W. Robinson, C. L. Mustoe, N. G. White, A. Brown, A. L. Thompson, P. Kennepohl, P. D. Beer, *J. Am. Chem. Soc.* **2015**, *137*, 499.
[46] P. Metrangolo, H. Neukirch, T. Pilati, G. Resnati, *Acc. Chem. Res.* **2005**, *38*, 386.
[47] P. Politzer, P. Lane, M. C. Concha, Y. Ma, J. S. Murray, *J. Mol. Model.* **2007**, *13*, 305.
[48] C. B. Aakeröy, M. Fasulo, N. Schultheiss, J. Desper, C. Moore, *J. Am. Chem. Soc.* **2007**, *129*, 13772.
[49] I. Alkorta, F. Blanco, M. Solimannejad, J. Elguero, *J. Phys. Chem. A* **2008**, *112*, 10856.
[50] A. C. Legon, *Angew. Chem. Int. Ed.* **1999**, *38*, 2686.
[51] J. P. M. Lommerse, A. J. Stone, R. Taylor, F. H. Allen, *J. Am. Chem. Soc.* **1996**, *118*, 3108.
[52] Q. Li, X. Xu, T. Liu, B. Jing, W. Li, J. Cheng, B. Gong, J. Sun, *Phys. Chem. Chem. Phys.* **2010**, *12*, 6837.
[53] R. S. Mulliken, *J. Am. Chem. Soc.* **1950**, *72*, 600.
[54] C. Wang, D. Danovich, Y. Mo, S. Shaik, *J. Chem. Theory Comput.* **2014**, *10*, 3726.
[55] T. Clark, *WIREs Comput. Mol. Sci.* **2013**, *3*, 13.
[56] P. Politzer, J. S. Murray, T. Clark, *Phys. Chem. Chem. Phys.* **2013**, *15*, 11178.
[57] C. Walbaum, M. Richter, U. Sachs, I. Pantenburg, S. Riedel, A.-V. Mudring, G. Meyer, *Angew. Chem. Int. Ed.* **2013**, *52*, 12732.
[58] J. Martí-Rujas, L. Meazza, G. K. Lim, G. Terraneo, T. Pilati, K. D. M. Harris, P. Metrangolo, G. Resnati, *Angew. Chem. Int. Ed.* **2013**, *52*, 13444.
[59] N. K. Beyeh, F. Pan, K. Rissanen, *Angew. Chem.* **2015**, *127*, 7411.
[60] G. Wang, Z. Chen, Z. Xu, J. Wang, Y. Yang, T. Cai, J. Shi, W. Zhu, *J. Phys. Chem. B* **2016**, *120*, 610.
[61] D. Quiñonero, I. Alkorta, J. Elguero, *Phys. Chem. Chem. Phys.* **2016**, *18*, 27939.
[62] Y. Mo, *J. Chem. Phys.* **2003**, *119*, 1300.
[63] Y. Mo, L. Song, Y. Lin, *J. Phys. Chem. A* **2007**, *111*, 8291.
[64] Y. Mo, L. Song, W. Wu, Z. Cao, Q. Zhang, *J. Theory Comput. Chem.* **2002**, *1*, 137.
[65] Y. Mo, S. D. Peyerimhoff, *J. Chem. Phys.* **1998**, *109*, 1687.
[66] Y. Mo, J. Gao, *Acc. Chem. Res.* **2007**, *40*, 113.
[67] V. Pophristic, L. Goodman, *Nature* **2001**, *411*, 565.
[68] C. Wang, F. Ying, W. Wu, Y. Mo, *J. Am. Chem. Soc.* **2011**, *133*, 13731.
[69] E. J. Cocinero, P. Çarçabal, T. D. Vaden, J. P. Simons, B. G. Davis, *Nature* **2011**, *469*, 76.
[70] S. Grimme, *J. Comput. Chem.* **2006**, *27*, 1787.
[71] S. Grimme, J. Antony, S. Ehrlich, H. Krieg, *J. Chem. Phys.* **2010**, *132*, 154104.
[72] S. F. Boys, F. Bernardi, *Mol. Phys.* **1970**, *19*, 553.
[73] M. W. Schmidt, K. K. Baldridge, J. A. Boatz, S. T. Elbert, M. S. Gordon, J. H. Jensen, S. Koseki, N. Matsunaga, K. A. Nguyen, S. Su, T. L. Windus, M. Dupuis, J. A. Montgomery, *J. Comput. Chem.* **1993**, *14*, 1347.
[74] Y. Zhao, D. G. Truhlar, *Theor. Chem. Acc.* **2008**, *120*(1–3), 215.
[75] A. Bauzá, I. Alkorta, A. Frontera, J. Elguero, *J. Chem. Theory. Comput.* **2013**, *9*, 5201.
[76] S. Kozuch, J. M. L. Martin, *J. Chem. Theory Comput.* **2013**, *9*, 1918.
[77] R. A. Bachorz, F. A. Bischoff, S. Hofener, W. Klopper, P. Ottiger, R. Leist, J. A. Frey, S. Leutwyler, *Phys. Chem. Chem. Phys.* **2008**, *10*, 2758.
[78] S. Grimme, *J. Chem. Phys.* **2003**, *118*, 9095.

Received: 23 July 2017
Revised: 28 August 2017
Accepted: 5 September 2017
Published online on 26 September 2017